3-D SIMULATION OF TURBULENT THERMALS USING LARGE EDDY SIMULATION

Jaswant SINGH[1], Juichiro AKIYAMA[2], Mirei SHIGE-EDA[3]

[1]Student member of JSCE, Graduate Student, Dept. of Civil Engineering, Kyushu Institute of Technology (1-1 Sensui cho, Tobata ku, Kitakyushu 804-8550, Japan)

[2]Member of JSCE, Ph.D., Professor, Dept of Civil Engineering, Kyushu Institute of Technology

[3]Member of JSCE, Dr. Eng., JSPS Research Fellow, Dept. of Civil Engineering, Kyushu Institute of Technology.

A three-dimensional Large Eddy Simulation (LES) model investigating the motion of turbulent axisymmetrical as well as line thermals is presented. The model governing equations are spatially filtered 3-dimensional Navier-Stokes equations and Mass Transport equation. Space derivatives are calculated by Compact Finite Difference Scheme (CFDS) and time derivatives are calculated using Crank-Nicholson method. The turbulence generated is taken care of by eddy viscosity calculated using the modified Smagorinsky model, which includes buoyancy term. The comparison of simulated thermal characteristics like shape, size, buoyancy and mass center velocity for axisymmetrical as well as line thermals, with reported experimental results are found in reasonably good agreement. The behavior of thermal with different length to width ratio (ζ) of initial conditions, is also investigated using this model. It is observed that if the value of ζ is more than 5, the thermal's behavior is closer to a line thermal of infinite length.

Key Words: *Axisymmetrical thermal, LES, Smagorinsky model, fluid particle flows*

1. INTRODUCTION

Study of thermals is of great importance in many areas like dumping of dredged materials into the sea, artificial land reclamation, disposal of industrial wastes, water quality studies and study of assessment of impact of such projects on marine environment etc. Such practices raise not only water quality concerns associated with potential loss of contaminants to the water column during disposal, but also engineering challenge related to the ability of barges or scows to accurately place dredged and capping materials within the targeted area. However, the process of the settling of dumped particles and their spreading on the sea bottom, is not yet fully understood for a through evaluation of the impact of such projects on the environment.

Many studies on thermals are reported. For instance, Baines and Hopfinger[1)] conducted experiments on axisymmetrical conservative heavy thermals and showed that the effect of large density is confined to the region near the source. Maxworthy[2)] conducted experiments on conservative axisymmetrical thermals produced by forcing a mass of fluid through an orifice. They estimated the drag coefficient to be in the range of 0.09 ± 0.01 by taking slope of non-dimensional velocity versus depth data. Ruggaber[3)] conducted a series of experiments on axisymmetrical non-conservative thermals and showed that the wake formation is highly dependent on the way of releasing the thermal fluid. Buhler and Papantoniou[4)] proposed a relationship for the growth rate and velocity of suspension axisymmetrical thermals, which is applicable in, swarm phase also. Noh and Fernando[5)] conducted experiments on 2-D particle thermals and developed a relationship for the critical depth at which the thermal transits into swarm phase.

Sanchez et el.[6)] conducted experiments and performed simulations on conservative axisymmetrical thermals. But their simulation underestimated the observed thermal velocity at early stages and overestimated it in later stages and vice-versa in case of thermal half width. Li and Zang[7)] developed a 3-D numerical model using conservative characteristic based scheme. They applied their model to axisymmetrical and line thermals and produced reasonable results. Li[8)] used a 3-D model based on NS equations and mass

transport equations to simulate axisymmetrical non-conservative thermals. The author used Prandtl mixing length model to calculated eddy viscosity. The model did not simulate the double peak distributions for large particles (0.6-1.18mm). Akiyama et el.[9] and Ying et el.[10] investigated motion of 2-D non-conservative and conservative thermals from falling to spreading, experimentally as well as numerically with and without imposing a turbidity fence.

In this study, we have developed a 3-D numerical model for simulation of thermals using LES. The governing equations are solved using Compact Finite Difference Scheme CFDS[11] along with Crank-Nicholson fractional step method. The model is verified through reported experimental data for axisymmetrical[3),6)] thermals as well as line[9),10)] thermals. In both kinds of thermals, the results of the model are in reasonably good agreement with the experiments.

The behavior of thermal with different length to width ratio of initial conditions is also investigated using this model. This ratio ζ is an important parameter in designing the dimensions of the hopper used for dumping the materials into sea. It is observed from simulations that if the value of ζ is more than 5, the thermal's behavior is closer to a line thermal of infinite length.

2. MODEL DEVELOPMENT

In the development of the model, several assumptions are made. The particle phase is treated as fluid phase and the drift velocity between fluid and particles is assumed to be the settling velocity of the particles. The second assumption is that the Boussinesq assumptions are assumed to be valid.

(1) Governing equations

The governing equations are three-dimensional, incompressible Navier-Stokes equations and Mass Transport equations. Following the classical LES approach, the flow variables are decomposed into large-scale, resolvable and subgrid-scale non-resolvable parts using grid filtering.

$$\frac{\partial U_i}{\partial x_i} = 0 \tag{1}$$

$$\frac{\partial U_i}{\partial t} + U_j \frac{\partial U_i}{\partial x_j} = -\frac{1}{\rho_a}\frac{\partial P}{\partial x_i} + \nu \frac{\partial^2 U_i}{\partial x_j^2} + \frac{\partial}{\partial x_j}\left(-\overline{u_i' u_j'}\right) + g_i \frac{\Delta\rho}{\rho_a} \tag{2}$$

$$\frac{\partial C}{\partial t} + \left(U_i + V_{si}\right)\frac{\partial C}{\partial x_i} = \frac{\partial}{\partial x_i}\left(-\overline{u_i' c'}\right) \tag{3}$$

where U_i = mean velocity component in the x_i direction, P = pressure in excess of the hydrostatic pressure at reference ambient density ρ_a, ρ = thermal fluid density, $\Delta\rho$ = density excess $(=\rho-\rho_a)$, ν = kinematic viscosity, g_i = acceleration due to gravity in the x_i direction, u_i' = non-resolved component of velocity, C= volumetric concentration of particles or dense fluid, D = diffusivity (ν/S_c), S_c = Schmidt number, c' = non-resolved component of concentration; $\overline{u_i' u_j'}$ = sub grid correlation terms between non-resolved components of velocities due to the grid-filtering, $\overline{u_i' c'}$ = subgrid correlation terms between non-resolved velocity component and non resolved concentration component, V_{si} = settling velocity of a particle in the x_i direction and is computed by Rubey's equation given as;

$$V_{si} = \sqrt{s g_i d}\left(\sqrt{\frac{2}{3} + \frac{36\nu^2}{s g_i d^3}} - \sqrt{\frac{36\nu^2}{s g_i d^3}}\right) \tag{4}$$

where d = particle diameter, ν = kinematic viscosity and s = submerged specific density of particle. $-\overline{u_i' u_j'}$ can be expressed as;

$$-\overline{u_i' u_j'} = \nu_t\left(\frac{\partial U_i}{\partial x_j} + \frac{\partial U_j}{\partial x_i}\right) - \frac{2}{3}k\delta_{ij} \tag{5}$$

where ν_t = sub grid scale eddy viscosity; k = turbulent kinetic energy; δ_{ij}= Kronecker delta function. The last term in Eq. (5) represents the normal stresses and can be absorbed in the pressure terms of the momentum equations.

The sub grid scale eddy viscosity ν_t can be expressed by assuming that the sub-grid turbulent production includes a buoyancy term[12]. Therefore,

$$\nu_t = \left(Cs\Delta\right)^2\left(\left|\overline{S}\right|^2 - \frac{g_i}{\rho Sc_t}\frac{\partial\Delta\rho}{\partial x_i}\right)^{1/2} \tag{6}$$

where Δ = filter width, Cs = Smagorinsky constant and Sc_t = sub grid turbulent Schmidt number. The magnitude of large-scale strain is given by

$$\left|\overline{S}\right| = \left(2\overline{S}_{ij}\overline{S}_{ij}\right)^{1/2} \tag{7}$$

$$\overline{S}_{ij} = \frac{1}{2}\left(\frac{\partial U_i}{\partial x_j} + \frac{\partial U_j}{\partial x_i}\right) \tag{8}$$

The correlation term in Eq. (3) is generally expressed as;

$$-\overline{u_i' c'} = \frac{\nu_t}{Sc_t}\frac{\partial C}{\partial x_i} \tag{9}$$

Applying operator-splitting, Eq. (2) can be written as an advection-diffusion equation

$$\frac{\partial U_i}{\partial t}+U_j\frac{\partial U_i}{\partial x_j}=2\frac{\partial}{\partial x_j}\left[\left(\nu+\nu_t\right)\bar{S}_{i,j}\right] \quad (10)$$

and a pressure equation

$$\frac{\partial U_i}{\partial t}=-\frac{1}{\rho_a}\frac{\partial P}{\partial x_i}+g_i\frac{\Delta\rho}{\rho_a} \quad (11)$$

The pressure is computed by the Poisson equation, derived from algebraic manipulations of Eqs. (1) and (11) and is given below;

$$\nabla^2 P-(g_i\nabla\Delta\rho+\rho_a\nabla U_i)=0 \quad (12)$$

(2) Solution methodology

The equations to be solved are Eqs. (3), (10), (11) and (12). Solving Eq.10 by CFDS scheme, u, v and w are computed at intermediate time step (n+1/2), which is without inclusion of pressure terms. Using these velocities, Poisson equation Eq. (12) is solved for pressure using SOR method, calculating P for next time step. With the velocity and pressure known as above, Eq. (11) is solved for velocities at the next time level. Mass transport equation Eq. (3) is solved to update excess density. This process is repeated for reaching to next time level. The space derivatives are solved by Compact Finite Difference Scheme[11] (CFDS) and time derivatives are calculated using Crank-Nicholson fractional step method with CFDS. The imposed boundary conditions for velocity, pressure and concentration are

$$V_\tau=0,\quad V_n=0 \qquad \text{(Bottom boundary)}$$

$$\frac{\partial V_\tau}{\partial n}=0,\ \frac{\partial V_n}{\partial n}=0 \qquad \text{(Side boundaries)}$$

$$\frac{\partial V_\tau}{\partial n}=0,\quad V_n=0 \qquad \text{(Top boundary)}$$

$$\frac{\partial P}{\partial n}=0,\ \frac{\partial C}{\partial n}=0 \qquad \text{(All boundary)}$$

where τ and n denotes direction tangential and perpendicular to boundary respectively.

3. AXISYMMETRICAL THERMAL

The detail of thermal is schematically shown in **Fig.1** in which **Fig.1a** is depicting axisymmetrical thermal and **Fig.1b** depicts line thermal. Various parameters of thermal are A_0 = initial volume; W_0 = initial total effective gravity force ($=A_0\times g\times\varepsilon_0$); ε_0 = initial relative density difference ($=(\rho_0-\rho_a)/\rho_a$); H = half width of thermal; V = mass center velocity of thermal; h = total depth of ambient fluid; B = average effective gravity force and is calculated as ($=W_0/A$); A = volume of thermal at any distance z from origin; and x, y, z are directional ordinates respectively. In the following section, experimental conditions, computational conditions and results of the simulations are discussed.

Table 1 Experimental condition for thermals.

Case	Thermal fluid	s	d cm	ε_0	W_0 cm^4/sec^2
A1	Dyed Brine	------	-------	0.007	34.32
A2	Glass Bead	1.6	0.0264	0.06	23520.0
A3	Silt Solution	1.6	0.0010	0.167	23520.0
L1	Saline	------	-------	0.036	17640.0
L2	Glass Bead	2.47	0.0044	0.194	95000.0

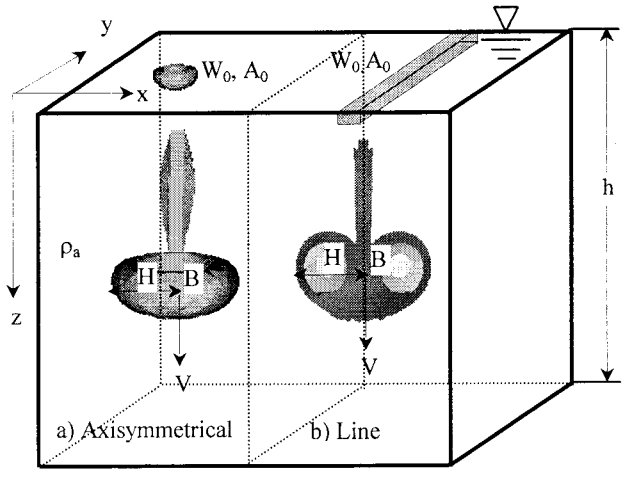

Fig. 1 Schematic diagram showing motion of thermals. (a: axisymmetrical thermal, b: line thermal)

(1) Experimental Conditions

Experimental conditions are presented in **Table 1.** Three cases of axisymmetrical thermal tabulated as A1, A2 and A3 respectively, and two cases of line thermal tabulated as L1 and L2, are simulated using the above-developed model. In case of conservative thermal A1, we have taken experimental data reported by Sanchez et el.[6] where initial volume A_0 was 10 cm^3. In case of non-conservative thermal cases A2 and A3, we have taken data from experiments conducted by Ruggaber[3] where A_0 was 55 cm^3.

(2) Computational Conditions

Free water surface is treated as horizontal rigid boundary. The grid size for all cases is 0.01m×0.01m×0.01m. Time step is 0.0025sec. The value of Smagorinsky Constant C_s is 0.21 and sub grid turbulent Schmidt number S_{ct} is 0.5. The computational domain for A1 is a grid of 31×31×31 points and for A2 and A3 cases 61×81×61.

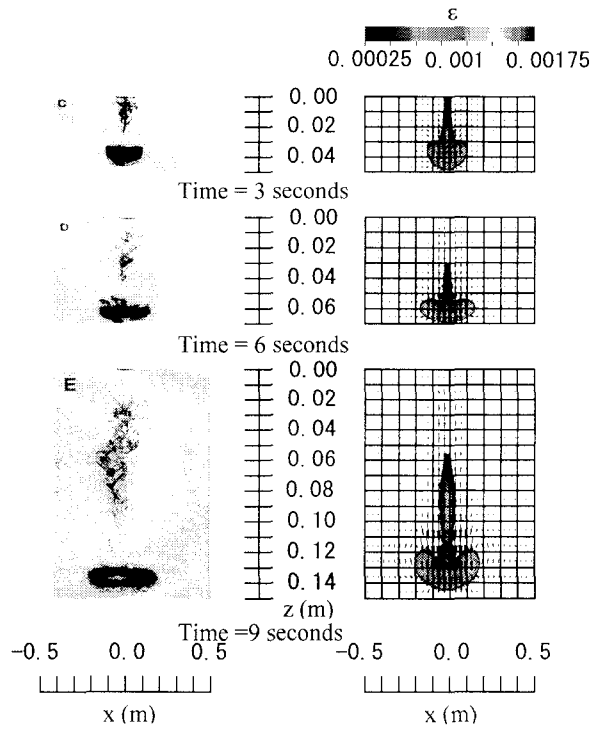

Fig.2 Comparison of experimental photographs and simulated axisymmetrical thermal for case A1.

(3) Results and Discussion

For qualitative analysis, the relative excess density ε contours along with velocity vectors for case A1 at 3, 6 and 9 seconds are compared with reported experimental photographs[6] and are shown in **Fig.2**. The Half width H and position of thermal are in satisfactory agreement with that of experiments.

For quantitative analysis, non-dimensionalised half width H^*, average effective gravity force B^* and mass center velocity V^* are presented as function of non-dimensionalised falling distance z^* in **Figs. 3~5**. Non-dimensional quantities are defined as $z^* = z/A_0^{1/3}$, $H^* = H/A_0^{1/3}$, $V^* = V/(W_0^{1/2}/A_0^{1/3})$. $B^* = B/(W_0/A_0)$. **Fig. 3** shows comparison of simulated and experimental H^* as a function of z^*. Half width for cases A1, A2 where the relative excess density ε is much lower are found in reasonable agreement with experiments. But in case of A3, where ε is higher than that of above two cases, simulated H^* is underestimated than that of experiments. This may be due to weak entrainment of ambient fluid into the thermal fluid as ε is higher at the time of release. So the expansion of thermal is poor and falls with a higher velocity. In **Fig.4** the comparison of simulated and experimental V^* as function of z^* for case A1, A2, and A3 is presented. The simulated values of V^* for cases A1 and A2 are in reasonable agreement with the experiments. In case of A3, the velocity is slightly overestimated than that of

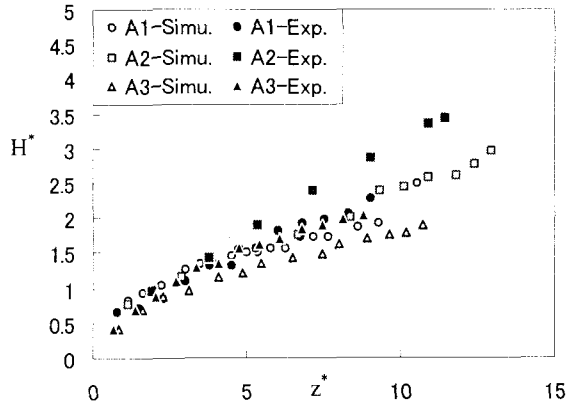

Fig.3 H^* as a function of z^*

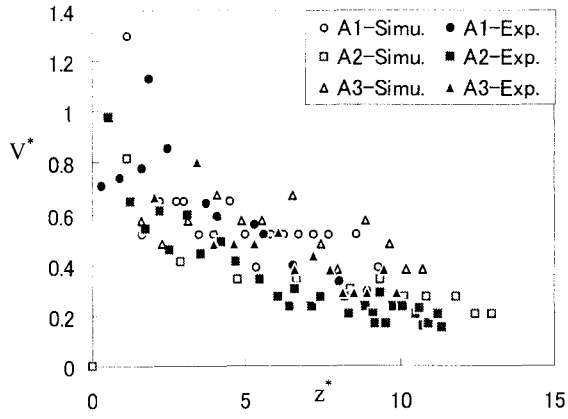

Fig.4 V^* as a function of z^*

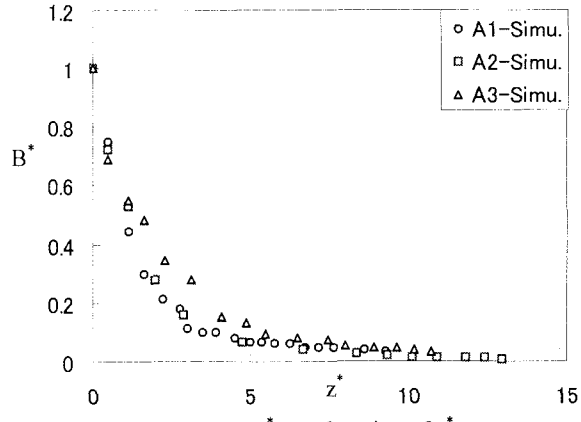

Fig.5 B^* as a function of z^*

experiments due to above said reason. **Fig. 5** shows the simulated B^* as a function of z^*. B^* is found to be decaying exponentially with z^*. Simulated B^* could not be compared with experimental data as in the reported experiments[3),6)] there was no experimental data corresponding to B^*.

4. LINE THERMAL

A line thermal is a special case of 3D thermal where thermal fluid is released from a line source parallel to the complete length of the flume.

(1) Experimental and computational conditions

The experimental conditions for line thermal are

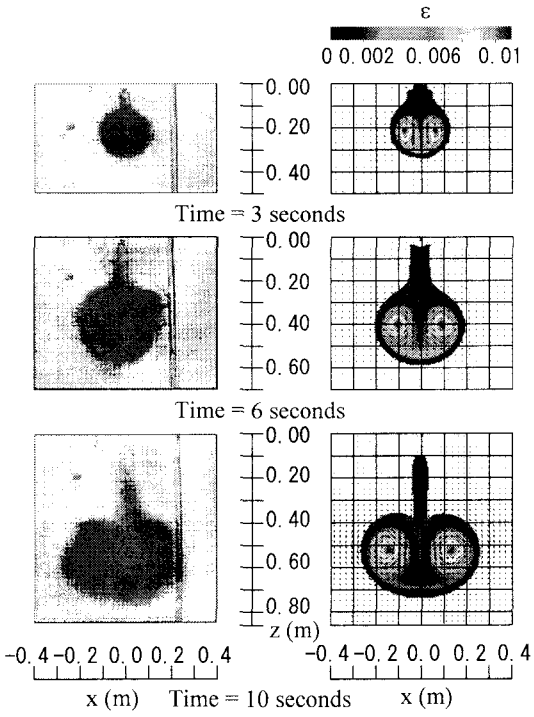

Fig.6 Comparison of experimental photographs and simulated line thermals.

tabulated in **Table 1**. One case of conservative thermal L1 and one case of non-conservative thermal L2 is simulated. We have taken experimental data reported by Ying et el.[10] for conservative thermals and Akiyama et el.[9] for non-conservative thermal. A_0 was taken 500 cm^3 for both the cases of line thermal. The computational domain for all cases of line thermal is $61 \times 85 \times 10$. Other computational conditions are same as in section 3(2).

(2) Result and Discussion

For qualitative analysis, simulated relative excess density difference ε contours are compared with experimental photographs at different time intervals as shown in **Fig. 6**. The shape of the simulated thermal is like an ellipse as also seen in the photographs. A strong internal circulating motion indicated by velocity vectors is also seen in the simulated thermals. The internal circulating motion is stronger than in axisymmetrical thermal (**Fig. 2**). The shape, size and position of the simulated and experimental thermal are in good agreement with that of the experimental photographs.

For quantitative analysis, H^*, B^* and V^* are plotted as a function of z^* for both cases. In **Fig.7** H^* is shown as a function of z^* and for both cases the computed results are in reasonably good agreement with the experimental values. The slope of H^* is higher than that in case of axisymmetrical thermals (**Fig. 3**). This indicates that the rate of ambient fluid

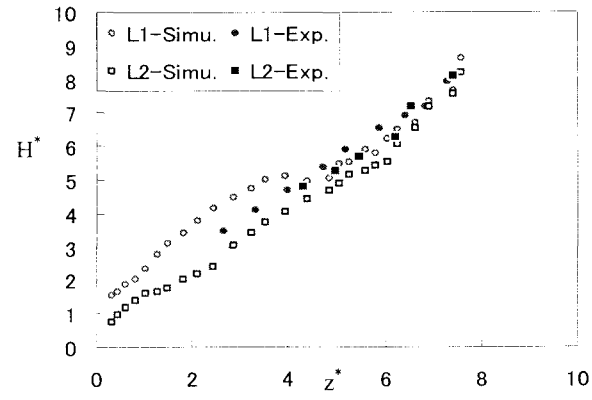

Fig.7 H^* as a function of z^*

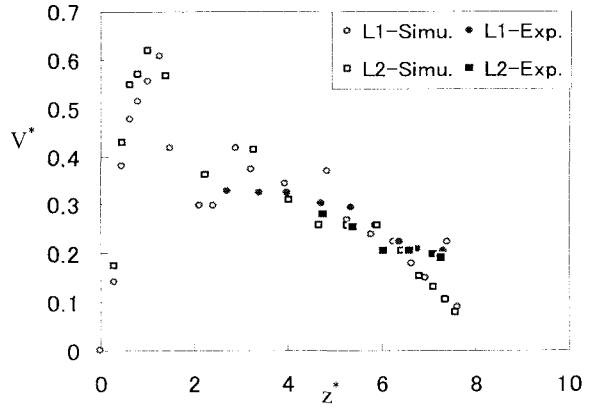

Fig.8 V^* as a function of z^*

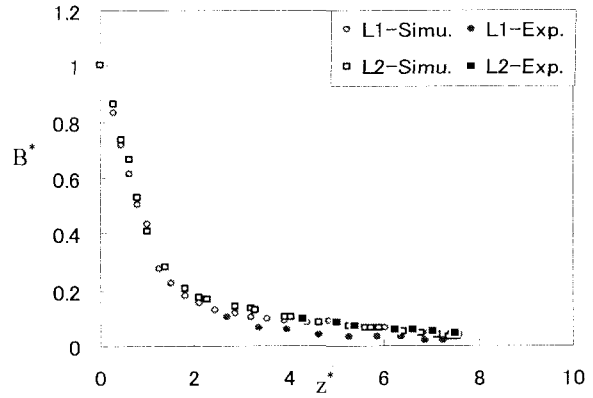

Fig.9 B^* as a function of z^*

entrainment is more in line thermals than in axisymmetrical thermal. The comparison of V^* as a function of z^* with experimental values is shown in **Fig. 8**. The reproduction of velocity for all cases is satisfactory. The simulated B^* as a function of z^* is compared with experimental values in **Fig. 9** and B^* is reproduced up to a considerable extent.

This model is used to simulate the behavior of thermals with different length α to width β ratio ζ ($=\alpha/\beta$), of initial conditions as shown in **Fig. 10.** For all cases of ζ (i.e.=1,3,5), initial W_0 per unit length and ε_0 were taken same as that of conservative axisymmetrical thermal case A1 listed in **Table 1**. Simulated thermal with different ζ is compared with simulated thermal of infinite length (i.e.$\zeta = \infty$)

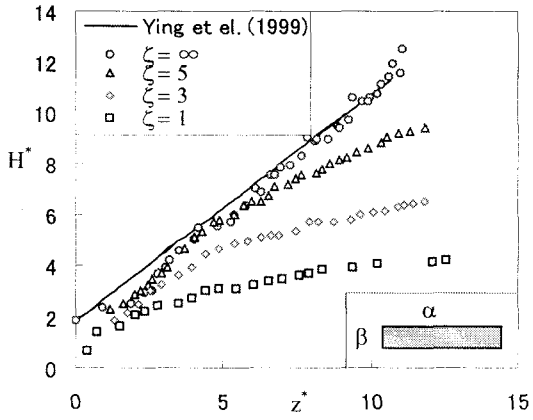

Fig.10 H^* as a function of z^*

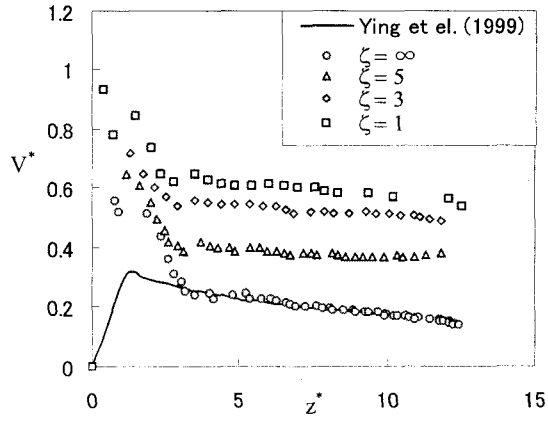

Fig.11 V^* as a function of z^*

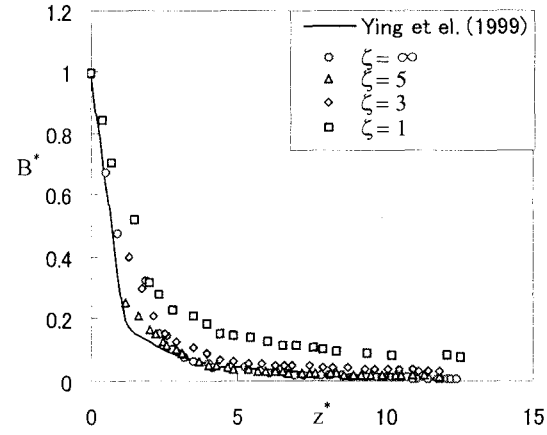

Fig.12 B^* as a function of z^*

and results of 2D thermal theory[10]. Quantitative analysis of thermal parameters H^*, V^*, B^* as a function of z^* is presented in **Figs 10~12** where line indicates the results of 2D thermal theory[10]. As shown in **Fig.10**, the slope of the H^* of the thermal increases as ζ increases and tends to be same as that of a 2D thermal. In **Fig.11** V^* as function of z^* is presented. V^* decreases as ζ increases. In case of B^* as presented in **Fig. 12,** the curve becomes closer to 2D thermal as the value of ζ approaches to 5.

5. CONCLUSIONS

A 3-D numerical model is developed for the simulation of thermals using LES. Eddy viscosity is calculated using modified Smagorinsky model and value of C_s and S_{ct} were taken as 0.21 and 0.5. Axisymmetrical and line thermals were simulated and compared with reported experimental data. The simulated results are found in reasonably good agreement with experiments. The behavior of thermal with different initial width to length ratio ζ is also investigated using this model.

AKNOWLEDGEMENT: This study was supported by the Grant-in-Aid for Science Research of the Ministry of Education and Culture, Japan under the Grant B (2), No. 1255149.

REFERENCES

1) Baines, W.D. and Hopfinger, E.J.: Thermals with large density difference, *Journal of Atmospheric Environment*, Vol.18, No. 6,pp.1051-1057,1984.
2) Maxworthy, T.: Turbulent vortex rings, *J. Fluid Mech.*, Vol.64, part 2, pp.227-239, 1974.
3) Ruggaber, G.J.: Dynamics of particle clouds related to open-water sediment disposal, Ph.D. thesis, Massachusetts Institute of Technology, USA, 2000.
4) Buhler, J. and Papantoniou, D. A.: Swarms of coarse particle falling through a fluid, *Environmental Hydraulics (Lee & Cheung (eds))*, Balkerma, Rotterdam, pp. 137-140,1991.
5) Noh, Y. and Fernando, H.J.S.: The transition in the sedimentation pattern of a particle cloud, *Phys. Fluid*, A5 (12), pp.3049-3055, 1993.
6) Sanchez, O., Raymond, D.J., Libersky, L. and Petschek, A.G.: The development of thermals from rest, *Journal of Atmospheric Sciences*, Vol.46, No.14, pp.2280-2292, 1989.
7) Li,C.W. and Zang, F.: Three-dimensional simulation of thermals using a split-operator scheme, *International Journal of Numerical Methods in Heat and Fluid Flow*, Vol.6, No.2, pp.23-35, 1996.
8) Li, C.W.: Convection of particle thermals, *Journal of Hyd. Research*, IAHR, Vol.35, No.3, pp.363-376, 1997.
9) Akiyama, J., Jha, A.K., Ying, X. and Ura, M.: Numerical study of 2-D particle clouds and effect of turbidity fences, *J. of Hydroscience and Hydraulic Eng.*, Vol. 19, No.1, pp.141-152, May, 2001.
10) Ying, X., Akiyama, J. and Ura, M.: Motion of dense fluid released into quiescent water with finite depth, *J. of Hydrau., Coast. Environ. Eng., JSCE*, No.635/II-49, pp.141-152, Dec., 1999.
11) Lele, S.K.: Compact finite difference schemes with spectral-like resolution, *Journal of Computational Physics*, 103, pp.16-42, 1992.
12) Edison, T. M.: Numerical simulation of the turbulent Rayleigh-Banerd problem using sub grid modeling, *J. Fluid Mech.*, Vol. 158, pp.245-268, 1985.

(Received September 30,2003)